Biochimica et Biophysica Acta 1859 (2017) 651–661

Contents lists available at ScienceDirect

Biochimica et Biophysica Acta

journal homepage: www.elsevier.com/locate/bbamem

Nanosecond pulsed electric fields trigger cell differentiation in *Chlamydomonas reinhardtii*

Fan Bai [a,*], Christian Gusbeth [b], Wolfgang Frey [b], Peter Nick [a]

[a] Botanical Institute, Karlsruhe Institute of Technology, Kaiserstr. 2, 76131 Karlsruhe, Germany
[b] Institute for Pulsed Power and Microwave Technology (IHM), Karlsruhe Institute of Technology, Campus Nord, 76344 Eggenstein-Leopoldshafen, Germany

ARTICLE INFO

Article history:
Received 31 August 2016
Received in revised form 22 December 2016
Accepted 4 January 2017
Available online 06 January 2017

Keywords:
Chlamydomonas reinhardtii
Nanosecond pulsed electric fields
Oxidative burst
Lipid peroxidation
Palmella formation

ABSTRACT

Nanosecond pulsed electric fields (nsPEFs) have great potential for biotechnological and medical applications. However, the biological mechanisms causing the cellular responses are still far from understood. We used the unicellular green algae *Chlamydomonas reinhardtii* as experimental model to dissect the immediate consequences of electroporation from the developmental cellular responses evoked by nsPEFs. We observe that nsPEFs induce a short-term permeabilization of the membrane, accompanied by swelling and oxidative burst. These response are transient, but are followed, several days later, by a second wave of oxidative burst, arrested cell division, stimulated cell expansion, and the formation of an immobile palmella stage. This persistent oxidative burst can be suppressed by specific inhibitor diphenyl iodonium (DPI), but not by the unspecific antioxidant ascorbic acid (Asc). Treated with natural and artificial auxins allow to modulating the cell cycle and cell expansion, and natural auxin can suppress the spontaneous formation of palmella stages. However, when administered prior to the nsPEFs treatment, auxin cannot mitigate the elevated formation of palmella stages induced by nsPEFs. We interpret our findings in terms of a model, where nsPEFs generate a developmental signal that persists, although the other immediate responses remain transient. This signal will initiate, several days later, a developmental programme comprising halted cell cycle, stimulation of cell expansion, a persistent activation of NADPH oxidase activity causing a second wave of oxidative burst, and the irreversible initiation of palmella stages. Thus, a short transient nsPEFs treatment can initiate a stable response of cellular differentiation in *Chlamydomonas reinhardtii*.

1. Introduction

Electroporation is widely used as a technique to transport biomolecules or other large molecules across the plasma membrane. In traditional electroporation, cells or tissues are exposed to pulses of microsecond to millisecond duration and low electric field strength. Under these conditions, the external electric field will cause hydrophilic pores (that are partially irreversible, partially reversible) in the plasma membrane due to massive rearrangement of phospholipid molecules in the membrane, leading to an increase of cell membrane permeability [1]. The increase in membrane permeability allows passage of ions and macromolecules, and electroporation can be used to introduce pharmacological compounds into the target cells. The genetic transformation of cells by electroporation represents probably the most widespread application, although it is not completely clear, how the DNA can pass the membrane [2,3]. Further technical applications are quite diverse and include the extraction of cellular ingredients [4], or even the prolongation of the shelf life for food [5].

During recent years, traditional electroporation has been complemented by nanosecond pulsed electric fields (nsPEFs). These pulses, characterised by high field strength (up to 300 kV/cm) and extremely short duration (in the nanosecond range), produce a wide variety range of interesting biological effects. What renders nsPEFs distinct is the fact that the electric field penetrates into the cell before it is dissipated by charging of the plasma membrane. This treatment will induce a transient increase of membrane permeability and therefore allows for a mild form of electroporation without affecting cell viability [6]. The magnitude of the transport of ions and molecules through the plasma membrane is lower for nsPEFs treatment when compared to traditional electroporation [7]. Nevertheless, cellular responses can be observed including calcium mobilization [8], cell swelling [9], cytoskeletal disintegration [10], and even apoptotic (i.e. not acute) cell death [11]. However, the biological mechanisms underlying these cellular responses are still poorly understood.

Formation of membrane pores can be reversible or irreversible, depending on pulsing parameters. However, even under conditions, where these pores are of transient nature, cellular integrity is temporarily

* Corresponding author.
E-mail addresses: baifan1215@aliyun.com (F. Bai), christian.gusbeth@kit.edu (C. Gusbeth), wolfgang.frey@kit.edu (W. Frey), peter.nick@kit.edu (P. Nick).

http://dx.doi.org/10.1016/j.bbamem.2017.01.007
0005-2736/

interrupted and this is presumably perceived as stress condition. It is, thus, useful to consider the biological responses elicited by nsPEFs from a stress physiological viewpoint. Although cellular stress can assume numerous different shapes, most of the early signals are shared. One of these central stress signals is oxidative burst, whose temporal and spatial signature allows the target cell to discriminate different stress types and to respond by activation of appropriate adaptive responses [12]. Oxidative burst is generally defined as the rapid production of large quantities of reactive oxygen species (ROS) in response to the stimulation of external environment [13]. The biological function of these ROS actively produced during the oxidative burst, such as superoxide anions (O_2^-), hydrogen peroxide (H_2O_2), and hydroxyl radicals ($\cdot OH$) [14,15], is to signal the incidence of a stress condition leading to responses in cell proliferation, differentiation, but in some cases also of programmed, apoptotic, cell death [16,17]. In biotic stress, ROS can also be employed to directly attack the invading pathogen [18]. In plant cells, ROS can be generated via a number of routes, such as the Mehler reaction in the chloroplast [19], the C_2 pathway of peroxisomes [14], or by a disbalanced electron transport system in the mitochondria [20,21]. While these sources of oxidative burst seem to be rather linked with cellular damage and are difficult to be controlled, the central source of signalling ROS in plant cells seems to be the plasma membrane located NADPH oxidase RboH (Respiratory burst oxidase Homolog), which is a central player in a broad range of plant stress responses (for review see [22,23]). To quantify the amplitude of oxidative burst, the so called MDA assay has been used extensively. This assay makes use of the fact that ROS oxidize double bonds of unsaturated fatty acids in membrane lipids (lipid peroxidation), yielding as products conjugated dienes, hydroperoxides, and malone dialdehyde (MDA), which can be quantified by a colorimetric assay [24]. However, superoxide, generated by RboH, is also used for signalling of the plant hormone auxin (through a receptor located at the outer face of the plasma membrane) and can enter the cytoplasm through aquaporins. Superoxide therefore links the stress response with a modulation of growth and proliferation [25]. One of the central targets for superoxide seems to be plant actin [26], which on the other hand is a central factor underlying membrane integrity. Disruption of membrane integrity would increase the penetration of superoxide into the cytoplasm, such that actin which is linked with the membrane could respond to nsPEFs [27]. This implied that nsPEFs should act on the actin cytoskeleton, and that the resulting response is evolutionarily ancient and therefore shared between animal and plant cells (and therefore also be present in the Chlorophyta including *Chlamydomonas*). In fact, nsPEFs induced the disintegration of the actin cytoskeleton in the cortex of tobacco cells, which was followed by a contraction of actin filaments towards the nucleus and a disintegration of the nuclear envelope [10]. Also in mammalian cells, the membrane permeabilization caused by nsPEFs not only caused osmotic imbalance and cellular swelling, but also a rapid disintegration of the actin cytoskeleton [9]. Whether these actin responses are accompanied by oxidative burst has not been, to the best of our knowledge, addressed so far. However, pulsed electric fields in the millisecond range have been reported to cause an oxidative burst lasting till about 60 min after pulsing, thus persisting much longer than the actual electropermeabilization of only 5 min [28].

To address, whether nsPEFs can modulate the balance between proliferation and stress responses, it is necessary to use experimental models with vigorous proliferation that are amenable to electropulse treatment, which is technically easier to achieve for unicellular systems rather than for multicellular organisms. The unicellular alga *Chlamydomonas reinhardtii* represents a suitable model for this purpose, since it strongly proliferates in both liquid culture or on agar medium and can be controlled by various environmental signals [29]. As part of the ancestral line for the land plants, it has been extensively studied as model organism for photosynthesis, gene expression [30,31], or for flagellar assembly and motility [32]. In addition, *C. reinhardtii* has been used as cellular factory for the production of biochemicals for food, aquaculture and pharmaceutical industries, or for recombinant proteins [33,34]. Although it is unicellular, this species is capable of distinct developmental responses. For instance, it can, in response to osmotic stress, shed the flagellae and produced the immobile so called palmella stage, that is ensheathed in a protective gelatinous matrix, thus recapitulating a situation that is normally seen during sexual reproduction that is triggered by depletion of nitrogen, and irradiation with blue light [35].

We therefore used this experimental model to investigate the role of oxidative burst for the cellular and developmental responses induced by nsPEFs. To dissect the acute consequences of electroporation from the developmental cellular responses triggered by the signalling elicited by nsPEFs, both short-term (over the first 2 h after the nsPEFs treatment), and long-term (over several days after the nsPEFs treatment) responses were investigated. The responses were monitored by quantifying cell size, mortality, optical density (OD), membrane permeability, and lipid peroxidation as readout for the amplitude of oxidative burst. To modulate the oxidative burst generated by nsPEFs, we used either diphenyl iodonium (DPI), a specific inhibitor of membrane-located NADPH oxidases [36], or the non-specific antioxidant ascorbic acid (Asc). Using this approach, we can show that nsPEFs induce a short-term permeabilization of the membrane, linked with a transient swelling and a transient oxidative burst. Although these responses vanish within the first 2 h after the pulse, they induce a developmental response which becomes manifest only several days later. This developmental response consists of halted cell cycle, stimulation of cell expansion, a strong oxidative burst, which is driven by the NADPH oxidase RboH, and the stimulation of palmella stages. Induction of a persistent oxidative burst by salinity stress can phenocopy the developmental response to nsPEFs. The transition point from cycling into cell expansion can be modulated by manipulation of auxin signalling, and auxin can also suppress the spontaneous transition into the palmella stage. However, auxin cannot suppress the induction of palmella formation by nsPEFs. We arrive at a working model, where the temporary permeabilization of the plasma membrane by nsPEFs treatment activates the membrane located NADPH oxidase RboH, generating apoplastic superoxide, which then triggers a developmental response whose biological context is adaptation to (osmotic) stress.

2. Material and methods

2.1. Cell cultivation

The microalgal strain used throughout this study was *Chlamydomonas reinhardtii* 137c, isolated in 1945 near Amherst, MA [37], obtained from the *Chlamydomonas* collection (www.chlamycollection.org). Cells were grown and maintained in 30 ml of fresh, sterilized Tris-Acetate-Phosphate (TAP) medium [38] in a 100 ml Erlenmeyer flask under a continuous white illumination provided by a custom-made light source consisting of a LED array placed on a cooler fabricated of aluminum and a power supply (VLP-2403; Voltcraft, Germany) and a fluence rate of 45 $\mu mol \cdot m^{-2} \cdot s^{-1}$ photosynthetically available radiation at 25 °C with continuous rotation of 150 rpm on an orbital shaker (KS260 basic; IKA Labortechnik, Staufen, Germany). To standardise culture growth, a standardised number of stationary cells was inoculated yielding an initial optical density (OD) of 0.05. Under these conditions, the duration of the cultivation cycle was 7 days (Fig. 1B). As backup, *C. reinhardtii* cells would also be streaked on the TAP medium solidified by 1.5% (w/v) agar and subcultured every 20 days.

2.2. Nanosecond pulsed electric fields (nsPEFs)

30 ml of algal suspensions were treated with nsPEFs in a treatment chamber (Fig. 1A). The custom-made treatment chamber consisted of two stainless steel electrodes with a diameter of 60 mm, oriented in parallel and separated by a gap integrated into a transparent polycarbonate

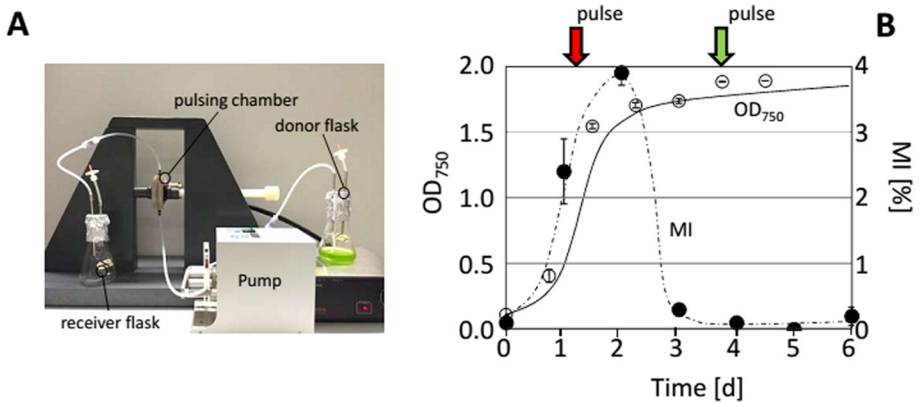

Fig. 1. Experimental set up and design of pulse treatment. A Device to administer nsPEFs. The cell suspension is pumped from the donor flask, the suspension is then passing through the pulsing chamber where cells experience the nsPEFs treatment and are collected in the receiver flask. B Timing of the pulse treatment (arrow) in relation to the physiological parameters of the culture. To study long-term responses, the pulse was administered 30 h after subcultivation (red arrow), to study short-term responses, the pulse was administered 4 d after subcultivation (green arrow). The time courses of OD750 as measure for cell density (open circles, solid line) and mitotic index (filled circles, dashed line) are shown. Data represent mean values, error bars se of three independent experimental replications. For the details of the nsPEFs treatment refer to Table 1. (For interpretation of the references to colour in this figure legend, the reader is referred to the web version of this article.)

housing. The details on the treatment chamber and the pulsed generator system were reported previously [4,39].

The cell suspensions passed the treatment chamber from the bottom via a sterilized silica rubber tubing driven by a peristaltic pump (Ismatec Ism 834C, Switzerland) at a constant flow rate of 6.38 $ml \cdot min^{-1}$. After passing the outlet at the top of the chamber, the suspension was collected in an empty, sterilized 100 ml Erlenmeyer flask sealed by a silicone plug. In this work, the transmission line pulse generator delivered rectangular pluses with a voltage amplitude of 8 kV, corresponding to an electric field strength of 40 $kV \cdot cm^{-1}$. The distance between the electrodes is 2 mm and the treatment volume is 0.5 ml. The frequency of the pulses was 4 Hz and the conductance was 1.4 $mS \cdot cm^{-1}$. Pulses were generated in durations of 25 ns and 50 ns, corresponding to specific input energies of 1 $J \cdot g^{-1}$ and 2 $J \cdot g^{-1}$, respectively (Table 1).

In this work, we investigated both, short-term, and long-term responses of *C. reinhardtii* to nsPEFs. To follow the short-term responses, the suspension was pulsed at day 4 after subcultivation (Fig. 1B, green arrow). To measure these immediate cellular responses, a high density was crucial to be able to measure the more subtle cellular aspects. We had therefore to conduct these measurements in a later stage of the cycle. To follow long-term responses, the suspension was pulsed at 30 h after subcultivation (when the cell was under exponential phase) (Fig. 1B, red arrow). This earlier time point (30 h) was required since the modulations required several days to become manifest, and otherwise would have shifted beyond the cultivation cycle, such that resulting loss of viability would affect the validity of the experiment. As negative control, the suspension was cultivated and treated the same way, just omitting the application of nsPEFs. After the pulse treatment, all samples were transferred back to the incubator till analysis at specific time points. When measuring short-term responses, 0 min indicated the condition prior to pulse treatment, and 4 min the earliest possible time point after the treatment, because the 30 ml of suspension required 4 min to pass the treatment chamber.

2.3. Mortality assay

To quantify viability, the membrane-impermeable dye Evan's Blue was used [40,41]. 1 ml of cell suspension was spun down in a 1.5 ml reaction tube (Eppendorf, Hamburg) at 2000 × *g* for 2 min (PICO 17, Thermo Scientific, Germany) before replacing the supernatant by 1 ml of 2.5% Evan's Blue (w/v, dissolved in double distilled water). After incubation for 5 min, the dye was removed by centrifugation at 2000 × *g* for 2 min. Then, 1 ml of fresh TAP medium was added and vortexed briefly to remove unbound dye. This was repeated until the supernatant was colourless. Finally, the cells were resuspended in 250 µl of fresh TAP medium. Aliquots of 20 µl were quantified in a hematocytometer (Fuchs-Rosenthal) under an ApoTome microscope (AxioImager Z.1; Zeiss, Germany) using a 63× oil immersion objective. Data represent mean values and standard errors of at least 1500 cells per experiment and three independent experimental series.

2.4. Quantification of short-term responses of membrane permeability

To visualise the transient permeabilisation of the plasma membrane due to the application of nsPEFs, the conventional fluorescent marker propidium iodide was not appropriate, because in *C. reinhardtii* the red autofluorescence by chlorophyll masks the propidium iodide signal. We therefore used the membrane impermeable dye Evan's Blue. The protocol for staining was the same as given above, but the dye was added at specific time intervals after pulsing (up to 120 min). Data represent mean values and standard errors of at least 1500 cells per experiment and three independent experimental series.

2.5. Quantification of cell volume

To get statistic information about changes in cell size, an automized particle counter system (CASY® Model TT System version 1.1, Roche Diagnostics GmbH, Germany) was employed. During preparatory studies, the reliability of this approach had been validated by comparison with

Table 1
Basic parameters of nanosecond pulsed electric fields (nsPEFs).

	Field strength	Pulsed duration	Conductivity	Pump speed	Frequency	Pulse number	Input energy
Parameter 1	40 $kV \cdot cm^{-1}$	25 ns	1.4 $mS \cdot cm^{-1}$	40 rpm	4 Hz	18.8	1 $J \cdot g^{-1}$
Parameter 2	40 $kV \cdot cm^{-1}$	50 ns	1.4 $mS \cdot cm^{-1}$	40 rpm	4 Hz	18.8	2 $J \cdot g^{-1}$

direct measurements using bright-field microscopy. To exclude that particle debris would cause undesired background, each measurement was preceded by a cleaning procedure, whereby the measuring capillary was flooded by 10 ml of CASY® buffer (Roche Diagnostics) following the instructions of the producer. This step was repeated until the cell counts in the sample were below 200 per ml, before a new sample was measured. Aliquots of 50 μl of *C. reinhardtii* cell suspension were diluted in 10 ml of buffer and measured, collecting the data by means of the CASY excel 2.4 Software. Data represent mean values and standard errors from three independent experimental series. Volumes were inferred from the size distribution based on the assumption that the cells are spherical.

2.6. Quantification of lipid peroxidation by malone dialdehyde (MDA)

To quantify lipid peroxidation as readout for oxidative burst, the reaction product MDA was measured making use of the reaction between MDA and 2-thiobarbituric acid (TBA) yielding a coloured adduct following a protocol published for plant cells [42] with minor modification: 1 ml of cell suspension was filled into an empty and preweighed reaction tube (2.0 ml, Eppendorf, Hamburg), spun down for 4 min at 8000 × *g*, and then the supernatant was removed. By weighing the filled tube again, fresh weight of the cells was determined, and then the cells were shock-frozen in liquid nitrogen. A sterilized steel bead was added and then the frozen tissue was homogenised twice by a Tissuelyser (Qiagen, Retsch, Germany) at 18 Hz for 30 s. After addition of 1 ml 0.1 M phosphate buffer (pH 7.4) and centrifugation at 8000 × *g* for 4 min, 200 μl of the supernatant were transferred to a mixture containing 750 μl of 20% (v/v) acetic acid, 750 μl of 0.8% (w/v) TBA, 200 μl of Milli-Q water, and 100 μl of 8.1% (w/v) sodium dodecyl sulfate (SDS). As blank, the 200 μl of supernatant was replaced by an equal volume of 0.1 M phosphate buffer. Subsequently, both specimen and blank were incubated at 98 °C for 1 h. After cooling down to room temperature, the absorbance at 535 nm was measured in a UV–Vis Spectrophotometer (Uvikon XS, Goebel Instrumentelle Analytik GmbH, Germany) and corrected against the absorbance at 600 nm monitoring unspecific background. The content of MDA expressed $\mu M \cdot g\ FW^{-1}$) could be calculated from the corrected absorbance at 535 nm using an extinction coefficient of 155 $mM \cdot cm^{-1}$. Data represent mean values and standard errors from three independent experimental series.

2.7. Inhibitor experiments

To understand the role of NADPH-oxidase dependent oxidative burst stress, the inhibitor diphenyl iodonium (DPI) (2 μM, Sigma-Aldrich, Germany) and the general antioxidant ascorbic acid (5 mM, Sigma-Aldrich, Germany) were added 30 min before the pulse treatment (at 30 h after subcultivation). During preparatory experiments, different concentrations of DPI and ascorbic acid had been tested, and the concentrations were chosen such that adverse effects on cell viability were avoided. For higher concentrations of ascorbic acid, we observed a conspicuous loss of viability, such that the concentration was adjusted to 5 mM. As DPI is not readily soluble in water, and other possible solvents such as dimethyl formamide, are toxic to *Chlamydomonas*, DMSO was used as solvent with the minimal side effects. However, to account for potential ROS scavenging by DMSO, we designed our experiment such that a solvent control was included to account for this scavenging effect. Therefore, as negative control, samples with the respective solvent in the same final concentration (0.01% DMSO for DPI, water in case of ascorbate) were prepared and processed in the same manner. Data represent mean values and standard errors from three independent experimental series. To assess the effect of auxins on proliferation, the natural auxin indole acetic acid (IAA, Fluka, Buchs; Switzerland), along with the artificial auxins 1-naphthalene acetic acid (NAA, Sigma-Aldrich, Neu-Ulm; Germany), and 2,4-dichlorophenoxyacetic acid (2,4-D Sigma-Aldrich, Neu-Ulm; Germany) were added at the time of subcultivation in a final concentration of 10 μM. To probe a potential effect of natural auxin (IAA) on nsPEFs induced palmella formation, 10 μM of IAA were added to the cells 30 min prior to the pulse treatment (at 30 h after subcultivation).

2.8. Statistical analyses

All experiments were performed in three independent experimental series. The data represent in mean values and standard errors. The results of three replicate were carried out using Microsoft Office Excel Software (version 2007). The statistic test presented in $^{*}P = 0.05$, $^{**}P = 0.01$.

3. Theory

3.1. Reactive oxygen species as developmental signals

Over many years, reactive oxygen species (ROS) have been merely understood as result of deregulated redox balance and, thus, as indication for cellular damage [43]. Meanwhile, it has become clear that ROS fulfill a second, positive, role as signals that orchestrate the cellular adaptation to stress. If something acts as a signal, its production and decay must be regulated. In fact, a specific group of NADP(H) oxidases located in the plasma membrane have emerged as central tool for "deliberate" ROS release in plants (for review see [44]). This group of enzymes, called RboH (for Respiratory burst oxidase Homolog) generates superoxide by partial reduction of oxygen, and is activated by different stress conditions, including ionic and osmotic stress as well as biotic factors. Interestingly, a certain ground level of superoxide is also required for normal growth and development. For instance, the signalling of the central plant hormone auxin requires superoxide to activate small G-proteins of the Rac/Rop family that will subsequently activate the important signalling hub phospholipase D [25]. This molecular link between stress and auxin signalling provides a mechanism to explain how ROS can modulate important biological functions, such as cell proliferation, differentiation and induction of programmed cell death, the plant version of apoptosis [16,17]. When superoxide is not consumed for auxin signalling, this will alter the activity of phospholipase D. Since the different products generated by phospholipase D can sequester different actin-associated proteins, such as the actin-capping proteins and the actin-depolymerization factors, stress-dependent stimulation of the RboH will modulate dynamics and organisation of cortical actin, which in turn is a central switch for arrest of the cell cycle and initiation of cell differentiation including programmed cell death as one of the possible outputs [26]. This sequence of events can be mitigated by addition of auxin, because this will recruit the otherwise excessive superoxide from RboH activation for auxin signalling, thus preserving dynamics and organisation of cortical actin.

3.2. Quantification of oxidative burst

To follow time courses for the cellular responses to nsPEFs, it is necessary to quantify them. Although it is possible to visualise superoxide by fluorescent dyes such as dihydrorhodamine 123 [45], it is experimentally demanding to quantify this based on quantitative image analysis. Moreover, the fluorescent detection is hampered by the strong autofluorescence of chlorophyll present in the green protist *C. reinhardtii*. As alternative, the downstream effect of superoxide can be quantified [46]. The superoxide anion generated by RboH is converted by superoxide dismutase into hydrogen peroxide, and hydrogen peroxide will further be converted into hydroxyl radicals in presence of divalent iron. Whereas hydrogen peroxide is not very reactive, hydroxyl radicals can extract hydrogen from fatty acids, triggering a radical chain reaction, which will culminate in the formation of MDA. At high temperature and low pH, MDA can react with TBA to produce a coloured adduct which can be quantified by a colorimetric assay (for review see [47]).

Since the formation of MDA involves a chain reaction, this assay can detect the presence of superoxide at high sensitivity. However, one should keep in mind that MDA can, in principle, be generated from other sources than lipids, such as degraded DNA. Although these alternative sources under physiological pH and temperature are negligible [47], we always included non-stressed control samples to determine the ground level of MDA prior to the stress treatment. If this condition is met, MDA can be used as a marker for lipid peroxidation and reliable indicator of oxidative stress.

4. Results

4.1. Short-term response of C. reinhardtii to nsPEFs

To investigate the short-term response of *C. reinhardtii* to nsPEFs, cells were subjected to pulse treatment at day 4 after subcultivation. Cell membrane permeabilization, cell diameter, and MDA content as measure for lipid peroxidation were measured before and over the first two hours after pulse treatment (Fig. 2).

Transient membrane permeabilization was measured as percentage of cells taking up the membrane-impermeable dye Evan's Blue added at the respective time after pulsing. In comparison to the control, a treatment with a pulse duration of 25 ns did not cause an obvious change in membrane permeability (Fig. 2A). In contrast, for a pulse duration of 50 ns, about 3% of cells took up Evan's Blue, when if the dye was added 5 min after pulsing treatment. From the subsequent decrease, the uptake extrapolated for shorter time points is likely to be higher, but due to experimental constraints (the time for the sample to pass the pulsing chamber) time points shorter than 5 min could not be measured. If the dye was added later, uptake was found to decrease until the membrane had become again completely tight 15 min after the pulse. To determine the time constant for this membrane resealing after the 50 ns pulsing, a first-order kinetics was assumed, such that the natural logarithms of the values could be approximated by linear regression (Fig. 2B). From the slope of this line, the time constant was estimated to be around $-0.2\ \mathrm{min}^{-1}$, and since the regression coefficient was very close to unity, this approximation by a model assuming a first-order kinetics of resealing was found to be valid.

To verify, whether this transient increase of membrane permeability would result in a temporary swelling of the cell, we followed cell diameter over the first two hours after pulsing (Fig. 2C). Whereas, in control samples, the average volume of cells showed only minor fluctuations during the experiment, both, pulsing at 25 ns and 50 ns, produced a rapid increase of volume, followed by a gradual decrease. This transient swelling was more pronounced for the 50 ns pulse, but also observed for the 25 ns pulse (here, the volume did not completely return to the initial level). Thus, the volume increase was found to monitor membrane permeability more sensitively as the Evan's Blue exclusion assay.

To find out, whether the transient permeabilization of the membrane would result in increased lipid peroxidation, we measured the content of MDA as stable end product of lipid conversion (Fig. 2D). Again, both treatments, pulsing at 25 ns and 50 ns, respectively, caused a rapid increase of MDA levels that reached a plateau from around 15 min after the pulse. This plateau was significantly higher for pulsing at 50 ns as compared to 25 ns. In summary, *C. reinhardtii* responds to nsPEFs by a rapid and transient increase of membrane permeability, accompanied by a transient volume increase, and a somewhat slower lipid peroxidation. These responses become more pronounced when the input energy is doubled by increasing the duration of the pulse from 25 ns to 50 ns.

4.2. Long-term response of C. reinhardtii to nsPEFs

The elevated membrane permeability observed immediately after the nsPEFs treatment was found to be transient with restoration of the

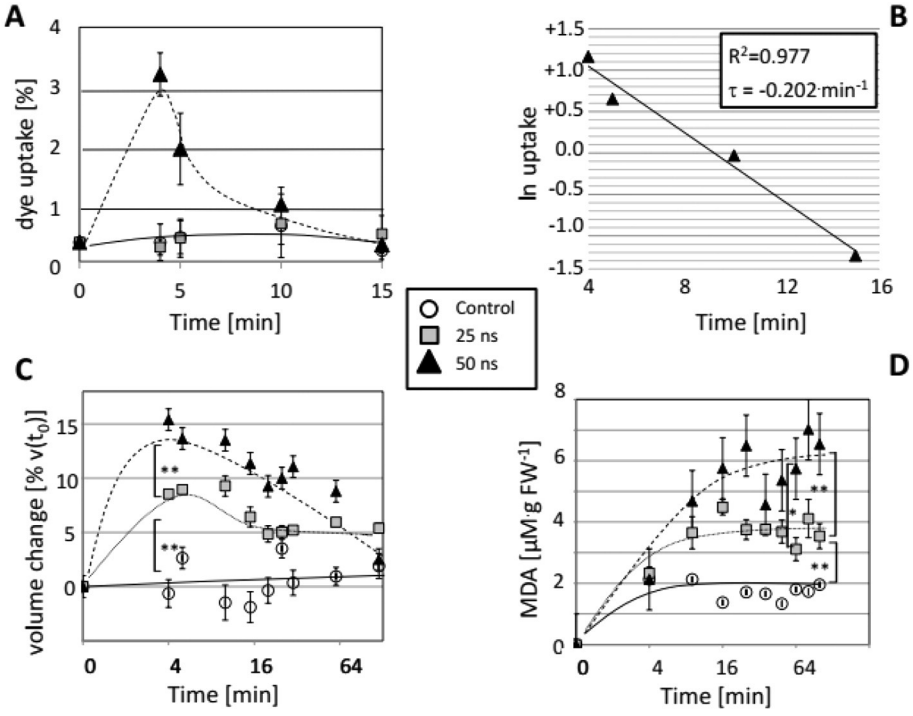

Fig. 2. Short-term response to pulse treatment. A Transient membrane permeabilization measured as percentage of cells taking up the membrane-impermeable dye Evan's Blue added at the respective time after pulsing. Details are given in Material and methods section. A sham sample (control) was compared to a pulse treatment with a pulse duration of 25 ns (grey squares), and a treatment with 50 ns (black triangles). B Determination of the time constant for resealing by plotting the natural logarithm of uptake values for the 50 ns treatment and determining a linear regression line. The slope of this line gives an estimate for the time constant of resealing of the membrane, the regression coefficient gives an estimate for the validity of the approximation by a model assuming a first-order kinetics of resealing. C Time course volume change (in % of start volume) in response to nsPEFs treatment. D Time course of lipid peroxidation in response to nsPEFs treatment. Data represent mean values, error bars se of three independent experimental replications. In order to resolve both, short and long time 20 points, the time is plotted on a log2 scale. Brackets indicate significant differences ($^{*}P = 0.05$, $^{**}P = 0.01$). For the details of the nsPEFs treatment refer to Table 1.

original situation within 2 h (Fig. 2A, C). In contrast, the stimulated lipid peroxidation as recorded by MDA remained on a plateau over the tested time interval (Fig. 2D). This led to the question, whether the short pulse treatment would cause any long-term response in *C. reinhardtii*. We therefore administered a nsPEFs treatment at 30 h after subcultivation, i.e. at the time of maximal proliferation activity. After pulsing, all cell suspensions returned to the incubator and cultivation continued till day 7, while optical density as measure of culture growth (OD_{750}), cell diameter, cell number, and MDA content were measured every day to detect potential long-term changes in response to the nsPEFs treatment (Fig. 3).

In fact, already from 18 h after the pulse treatment, the OD_{750} in both treatments, i.e. pulsing with 25 ns and 50 ns, was significant decreased compared to control, reaching a plateau that was significantly lower around two days earlier than in the wild type (Fig. 3A). Secondly, while the cell diameter in the control decreased sharply in consequence of cell division after 1 day of subcultivation and remained at this lower level till day 3, this drop was stopped immediately after pulsing, such that cell diameters in both treatments, i.e. pulsing with 25 ns and 50 ns, remained larger than those of the controls until day 4 of cultivation (Fig. 3B).

Since optical density depends on both cell number and cell size, cell numbers were determined directly by means of a cell counter, and from these numbers, mean cell cycle durations could be derived based on a model of exponential proliferation (Fig. 3C). These estimated doubling times were significantly increased by the nsPEFs treatment. Although both pulse treatments, with durations of 25 ns and 50 ns, could slow down the cell cycle compared to the control, the effect caused by pulse durations of 50 ns was significantly stronger than that for 25 ns.

Since nsPEFs had produced an increase of MDA that was persistent over the tested first two hours (Fig. 2D), we followed MDA content over the entire cultivation cycle. In the control, MDA levels increased during the proliferation phase and then decreased, when the culture passed from proliferation into cell expansion, and then remained low throughout the rest of the cultivation cycle (Fig. 3D). The pattern observed after pulsing at 25 ns or 50 ns, respectively, was initially very similar: a transient increase at day 2, followed by a decrease back to the initial levels prior to proliferation without significant differences to the control. However, whereas MDA levels remained low in the control from day 3, in the pulsed samples, MDA levels rose again reaching a second peak on day 6. This peak was substantial, especially for pulsing at 50 ns. Again, the amplitude of this long-term increase of MDA indicative of elevated lipid peroxidation was proportional to the input energy (caused by the difference in pulse duration). Thus, nsPEFs cause a persistent long-term increase in lipid peroxidation in *C. reinhardtii* although the membrane permeability caused by the pulse is transient.

4.3. The persistent response of lipid peroxidation to nsPEFs can be blocked by DPI

To get insight into the molecular mechanisms underlying the long-term response of lipid peroxidation in response to nsPEFs, 2 μM of DPI or 5 mM of Asc, respectively, were added 30 min before administering the pulse at the usual time, 30 h after subcultivation. Cell diameter, cell number, and MDA content were measured on day 5 after subcultivation, i.e. at a time point, where the long-term response of lipid peroxidation was increasing and had not yet reached saturation.

DPI as an inhibitor of the NADPH oxidase RboH clearly eliminated the production of MDA to the level observed in untreated controls on day 5 (Fig. 4A). In contrast, ascorbic acid, used as unspecific ROS scavenger, failed to mitigate the enhanced lipid peroxidation caused by the pulsing treatment (Fig. 4B), and in unpulsed controls as well as for 50 ns even stimulated the MDA levels compared to values seen in the absence of ascorbic acid.

The long-term effect of DPI (given 30 h after subcultivation) on cell expansion was different: whereas cell diameter at day 5 was significantly inhibited in the unpulsed control (Fig. 4C), such an inhibition was not observed in any of the pulsed samples. In contrast, the volume appeared to be even increased in presence of DPI (although this increase was only significant for a pulse duration of 50 ns. In contrast, cell number

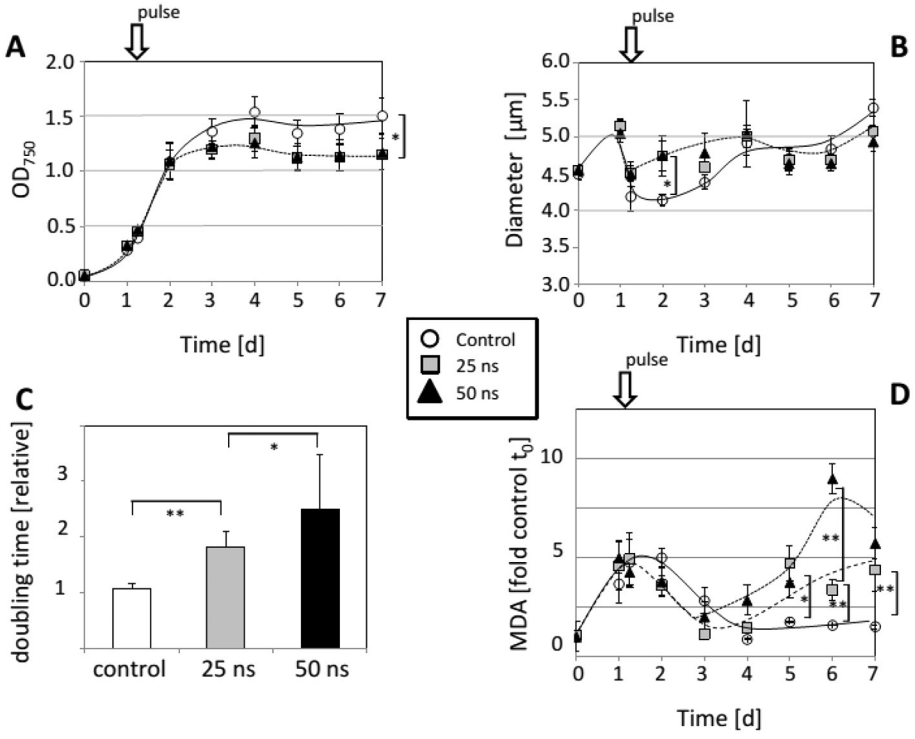

Fig. 3. Long-term response to pulse treatment. A Time course of optical density at 750 nm as measure for cell number. B Time course of cell diameter as measure for cell expansion. C Effect of nsPEFs treatment on doubling time as measure for cell cycle duration. D Time course of lipid peroxidation. Brackets indicate significant differences (*$P = 0.05$, **$P = 0.01$).

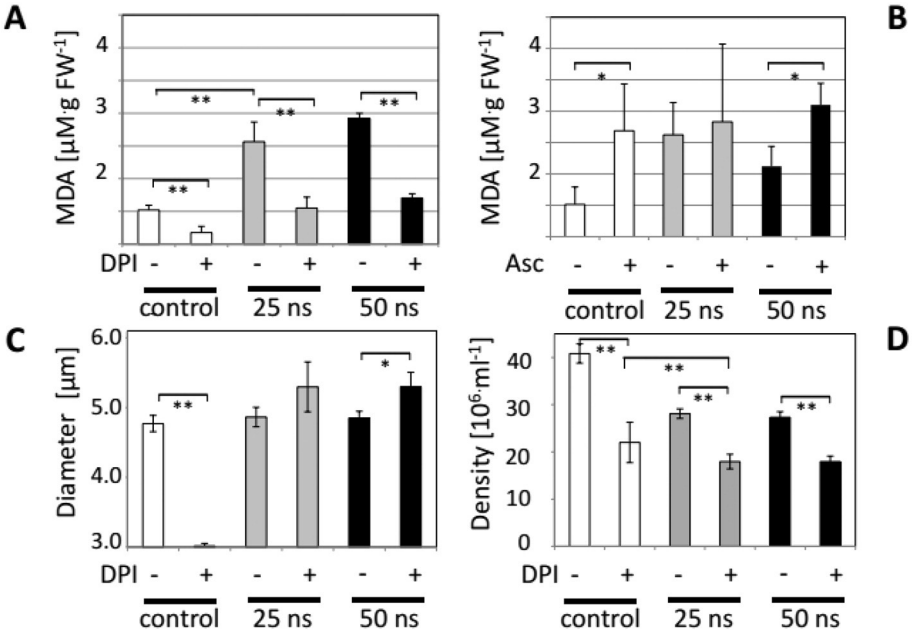

Fig. 4. Role of reactive oxygen species for the long-term response to pulse treatment. A Influence of DPI as inhibitor of the NADPH oxidase RboH was measured on the long-term response of lipid peroxidation. B Asc as general ROS scavenger was used as control for lipid peroxidation. C Cell diameter. D Cell density measured at day 5. DPI (2 µM) or Asc (5 mM) was added 30 min prior to administering the nsPEFs treatment at 30 h. Brackets indicate significant differences ($^{*}P = 0.05$, $^{**}P = 0.01$).

(as scored at day 5 of cultivation) was reduced in presence of DPI (Fig. 4D) indicating that DPI blocked cell division resulting in larger cells.

In addition, we observed a developmental response to nsPEFs (Fig. 5A). After pulsing at the 30 h after subcultivation, the frequency of palmella stage observed on day 5 of cultivation was significantly increased (Fig. 5A). Whereas the 25 ns treatment produced an increase by about 10% compared to the control, the 50 ns treatment yielded even 20% more palmella stages than the control (Fig. 5B).

4.4. Long-term response to salinity stress

Our previous experiments had shown an increase in the content of MDA indicative of stimulated lipid peroxidation several days after a nsPEFs treatment. This was accompanied by an increased frequency of palmella stages. To investigate, whether this developmental response was linked with lipid peroxidation, we tested the influence of salinity stress as independent stress factor known to stimulate lipid peroxidation. Cells were cultivated in the presence of different concentrations of NaCl, and OD_{750} was followed over 7 days, while MDA content and the frequency of palmella stage cells were determined on day 4.

The results show that cells were able to grow for all NaCl treatments, even at the highest tested concentration (100 mM NaCl). However, the lag phase was prolonged with increasing concentration of salt, whereas the transition to the stationary phase invariable occurred at day 4. As a result, the final OD_{750} was progressively reduced as the concentration of NaCl increased (Fig. 6A). In parallel, at the onset of stationary phase at day 4, both MDA levels and the incidence of palmella stages increased, when the concentration of NaCl was raised (Fig. 6B, C). These data show that the transition into the palmella stage was promoted also for a situation, when lipid peroxidation (as monitored by MDA) was stimulated through a stress factor different from nsPEFs.

4.5. Influence of natural and artificial auxins

Since the formation of the palmella stages occurred at the transition to the stationary phase, and since this transition can be modulated by the phytohormone auxin (IAA) in higher plant cells [48], we tested, whether the responses of *C. reinhardtii* to nsPEFs might be modulated by auxin as well. To investigate, whether these algal cells are responsive to auxins at all, in a first experiment, the natural auxin IAA was added, in

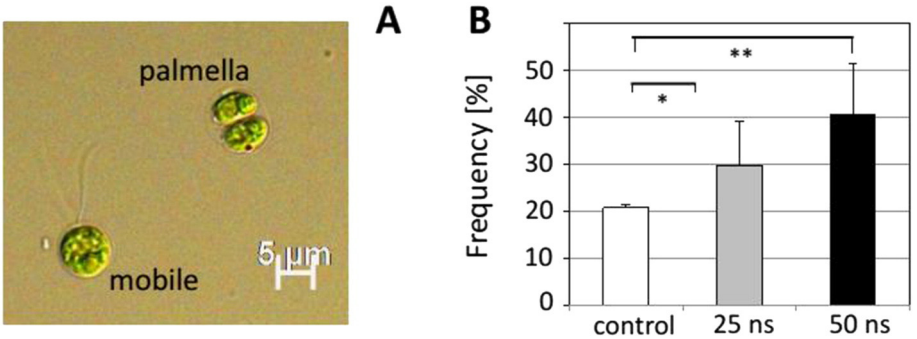

Fig. 5. Induction of palmella stage in response to pulse treatment. A Representative cells for the nsPEFs treatment. B Frequency of palmella stages at day 5 of the culture cycle under control condition, and following a nsPEFs treatment with 25 ns or 50 ns, administered at 30 h. Brackets indicate significant differences ($^{*}P = 0.05$, $^{**}P = 0.01$).

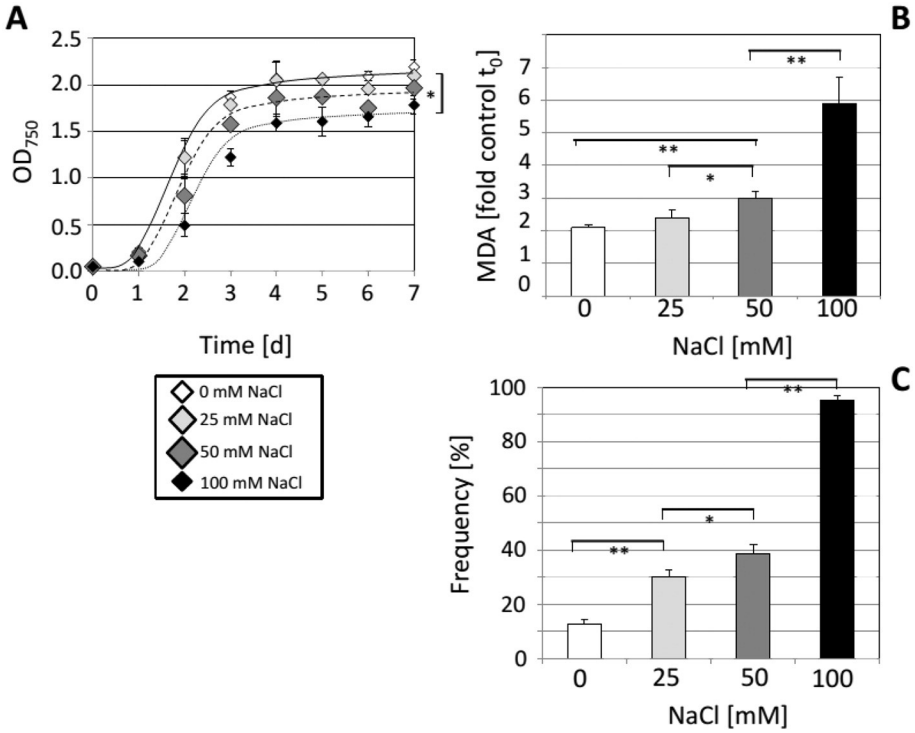

Fig. 6. Long-term response to salinity stress. A Time course of optical density at 750 nm as measure for cell number in presence of different concentrations of NaCl. B Lipid peroxidation measured at the onset of stationary phase at day 4. C Frequency of palmella stages at the onset of stationary phase at day 4. Data represent mean values, error bars se of three independent experimental replications. Brackets indicate significant differences ($*P = 0.05$, $**P = 0.01$).

parallel to the artificial auxins NAA and 2,4-D, and the OD_{750} was followed for each auxin treatment over the cultivation cycle of 7 days.

Compared to the control cultivated in the absence of auxin, IAA caused a significant reduction during the cycling phase of the culture, whereas it increased the OD_{750} during the phase of cell expansion in the second stage of the culture (Fig. 7A). The artificial auxin NAA strongly decreased OD_{750} at the beginning of the cycling phase, but had a slightly increasing effect throughout the subsequent stage (from day 2 to day 7), indicative for a block of cell proliferation and a stimulation of cell expansion. For the artificial auxin 2,4-D as well, an initial decrease was followed by a subsequent increase of OD_{750}. However, the time course was different: the inhibition of cycling was more persistent, and the increase of cell expansion was transient, indicative of a delayed transition into cell expansion. These experiments show that both natural and artificial auxins can modulate the developmental sequence of *C. reinhardtii*, whereby the effect of the two artificial auxins on the cycling and the expansion phase of the culture differ, as it also has been reported for cells from higher plants. It can therefore be concluded that *C. reinhardtii* is endowed with a functional system to sense and process auxin as a signal. We therefore wondered, whether the modulation of development by auxin might be able to interfere with the transition into the palmella stage. In controls, the formation of palmella stages at day 5 was completely suppressed by adding IAA at the time, where the pulse was administered (Fig. 7B). However, the promotion of palmella formation by the nsPEFs treatment could not be suppressed by IAA. This indicates that the differentiation process triggered by the nsPEFs treatment at 30 h, had already become irreversible at the time, when auxin was added.

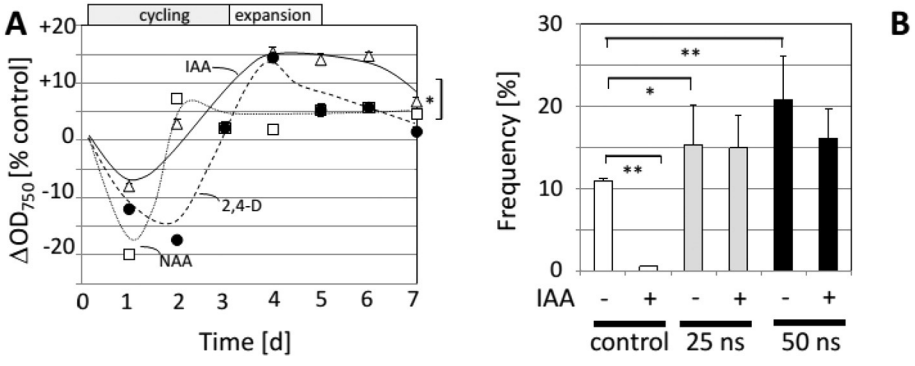

Fig. 7. Influence of natural and artificial auxins. A Time course for the modulation of optical density at 750 nm (plotted as differential with the value observed in the untreated control) caused by 10 μM of the natural auxin IAA, the artificial auxin NAA, or 2,4-D added at subcultivation. B Effect of natural auxin (IAA) on the frequency of palmella stages at day 5 of the culture cycle under control condition, and following a nsPEFs treatment with 25 ns or 50 ns, administered at 30 h. Data represent mean values, error bars se of three independent experimental replications. Brackets indicate significant differences ($*P = 0.05$, $**P = 0.01$).

5. Discussion

To get insight into potential cellular responses to the transient disruption of membrane integrity induced by nsPEFs, we investigated *C. reinhardtii* as ancestral plant cellular model with rapid proliferation, and observed not only immediate cellular changes in consequence of the formation of transient membrane pores, but also long-term responses that were expressed only several days after the pulse treatment.

5.1. Electroporation triggers lipid peroxidation

By quantification of MDA, we were able to detect a stimulation of lipid peroxidation after application of a nsPEFs (Fig. 2D). This lipid peroxidation developed from within a few minutes after the pulse and persisted for more than an hour. Strong pulsed electrical fields can generate reactive oxygen species even in cell-free medium [49] and this might directly lead to the peroxidation of lipids in the membrane. However, the fact that the lipid peroxidation initiates several minutes after the pulse, then proceeds over more than an hour (Fig. 2D), and then remained stable for more than a day (Fig. 3B), cannot be explained in terms of ROS generated directly by the electrical field, but strongly indicates a biological, rather than a physical, mechanism. Besides, the permeabilization induced by nsPEFs remains transient though: by measuring the uptake of the membrane impermeable dye Evan's Blue in a pulse-chase set-up, the resealing of the membrane can be followed and shown to follow a first-order kinetics (Fig. 2A, B). Even for a pulse duration of 50 ns, the initial leakage has completely dissipated within 10 min. The cellular swelling induced by this transient membrane permeabilization persists a bit longer, but it also remains transient - after a bit more than one hour cells have returned to their initial volume prior to the pulse (Fig. 2C). The fact that the cells can readjust their volumes, indicates that the contractile vacuole remains functional and that its activity is not irreversibly impaired by the nsPEFs.

Cellular swelling in response to nsPEFs has been observed repeatedly and a so called colloidal osmotic mechanism has been invoked to explain this phenomenon [50]. This phenomenon is caused by high molecular weight molecules (anionic colloids such as protens or organic phosphates) in the cytoplasm that are too big to pass through the pores created by the electric field, while simultaneously small solutes are able to enter the cell. The negative osmotic potential created by the trapped colloids will then drive cellular swelling in cells that are growing under isotonic conditions such as mammalian cells [51]. Whether colloidal osmosis occurs in *C. reinhardtii*, remains to be elucidated, but it is not needed here to explain the observed swelling: Like other freshwater protists, *C. reinhardtii* has to cope with a hypotonic medium which means that there is a continuous influx of water into the cell. The contractile vacuole, which is an organelle essential for all non-walled freshwater protists, has to continuously expel the penetrated water. Although the strain 137c used in the current study harbours a layered cell wall, this structure does not participate in osmoregulation, which is quite in contrast the cellulosic cell wall of higher plants. This can be inferred from the observation that in strains that are completely lacking a wall, such as CC-3395, the response of the contractile vacuole to osmotic challenge does not differ at all [52]. Thus, the most straightforward explanation for the slow, but complete readjustment of the original volume over the hour following the pulse treatment is the ongoing activity of the contractile vacuole. If the contractile vacuole were irreversibly inactivated by the nsPEFs treatment, the cells would burst, because the plasma membrane can maintain integrity only up to an extension of around 3% [53].

At a time, when the permeability to Evan's Blue had already vanished, and the transient swelling was already strongly declining, lipid peroxidation, as measured by accumulation of MDA, was still increasing (Fig. 2D), and these elevated levels of MDA persisted. Activation of oxidative burst by nsPEFs has been proposed as trigger for biological effects in mammalian cells, in concert with, or possibly even alternatively to, formation of nanopores [49]. Two mammalian cell lines that differed in their tolerance to nsPEFs treatment, also differed with respect to the accumulation of ROS, which again suggests a biological, rather than a physical mechanism. In our study, the oxidative burst occurs at a time, when the membrane is already resealed, which is consistent with a model, where oxidative burst acts downstream of nanopores formation. A potential mechanism would be the influx of calcium through the nanopores, as proposed from ratiometric measurements of the voltage-sensitive dye annine-6 in tobacco protoplasts challenged by nsPEFs [54], and patch-clamp studies of tobacco cells challenged by μsPEFs [55]. Whether calcium influx conveys the signal generated by the nanopores in *Chlamydomonas* as well, remains to be elucidated in future studies. In plant cells, elevation of cytosolic calcium will, through calcium dependent kinases, activate the NADPH oxidase RboH [56], which would provide a possible mechanism, how the early formation of nanopores would lead to a later oxidative burst. Alternatively, the membrane pores might simply allow the apoplastic superoxide, which is continuously generated by RboH, to leak into the cytosol, which in turn would divert a GTPase of the Rac family towards the activation of RboH, thus producing an autocatalytic loop [26,57]. This loop would also persist after resealing of the nanopores, because superoxide can enter the cell through aquaporins, such as the *Chlamydomonas* aquaporin homologues Major Intrinsic Protein 1 and 2 [57]. Again, a persistent oxidative burst would then act downstream of pore formation. It should be kept in mind that a temporal sequence and the existence of a plausible mechanism are still no hard proof for the hypothesis of ROS as second messengers for nsPEFs-dependent pore formation, because, still, the two events could act in parallel with different lag time and, thus, are not necessarily causally linked.

5.2. Oxidative burst is necessary and sufficient for long-term responses to nsPEFs

Among the primary cellular responses (membrane permeabilization, swelling, lipid peroxidation as readout for oxidative burst), lipid peroxidation was the most persistent, but 1.5 days after the pulse, no physiological imprints of the pulse treatment had remained (Fig. 3) giving the impression as if the cells had completely reversed to the *status quo ante*. This impression had to be revised, when we followed the development further and observed long-term changes including an induction of cell expansion, a delay of cell division, and a second wave of oxidative burst (Fig. 3). This was then followed by the formation of palmella stages (Fig. 5B), which in this species represents an adaptive response to osmotic stress [58]. In other words, the nsPEFs treatment activated a signalling chain that culminates in osmotic adaptation. This leads to two questions: Is the second oxidative burst induced by nsPEFs involved in the formation of palmella stage? Is the primary oxidative burst induced by nsPEFs necessary and sufficient for these developmental responses occurring several days later? To address this question, we added DPI, a specific inhibitor of NADPH oxidases [36], at 30 min before nsPEFs treatment to block the primary oxidative burst, and we then observed that both long-term oxidative burst generated by nsPEFs were suppressed (Fig. 4A), which suggested that the primary oxidative burst is necessary for the long-term effect. We also used ascorbate as a general ROS scavenger (Fig. 4B), but did not find a suppression indicative of a specific role the ROS generated by RboH that involved in the oxidative burst. The reason may be that ascorbate mainly acts on hydrogen peroxide generating hydroxyl radicals, a reaction that is especially pronounced in plants, where this reaction is catalysed by a ascorbate peroxidase and is absent from mammalian cells [59]. The results obtained with DPI were corroborated by experiments, where we activated RboH by salinity treatment (mimicking the natural condition which is encountered by this developmental response, palmella

formation), and we found that salinity stress could replace the nsPEFs treatment with respect to induction of the long-term oxidative burst and the formation of palmella stages (Fig. 6B, C). Thus, an oxidative burst (as that induced by nsPEFs) is necessary and sufficient to elicit long-term responses, such the second wave of oxidative burst, the arrest of cell division, the stimulation of cell expansion, and the formation of palmella stages.

5.3. Palmella formation versus cell division: a role for auxin signalling?

The oxidative burst observed in response to nsPEFs is accompanied by arrested cell proliferation, promoted cell expansion, and, a few days later, by the formation of palmella stages (Fig. 3). The same set of phenomena can be induced by salinity stress (Fig. 6), which represents the natural condition, for which this combination of responses had evolved. In higher plants, the superoxide generated by RboH is not only used as important stress signal, but is also consumed to convey signalling of the important plant hormone auxin. For this reason, in cells of higher plants, superoxide dependent stress responses can be mitigated by addition of auxin [26].

Whether the auxin pathway exists in the Green Algae had been a matter of debate over decades. The advent of genomics has allowed to probe for the presence of the respective genes in different taxa. This approach has revealed that *C. reinhardtii* harbours the components for auxin synthesis as well as the pgp1 type of auxin transporters, and components of signalling through the auxin-binding protein 1 [60]. In contrast, the PIN-type transporters, and the IAA/AXR-dependent signalling pathway seem to be absent.

We therefore tested first, whether auxins are active in modulating the development of *C. reinhardtii*. Our results (Fig. 7) clearly confirmed that both, the proliferation and the expansion phase, were regulated by auxins. However, the functional conservation extended beyond the mere existence of an auxin effect: In higher plants, the artificial auxin NAA stimulates mainly cell expansion, whereas the artificial auxin 2,4-D activates a different signalling pathway activating cell division [48]. This specific pattern was conserved as well, since the temporal progression of OD_{750} indicated a block of cell proliferation, and a stimulation of cell expansion for NAA, whereas 2,4-D delayed the transition from proliferation into cell expansion. Thus, we conclude that auxin signalling in *C. reinhardtii* is not only present, but also shares functional specificities with the auxin signalling from higher plants. Due to this high degree of conservation, it appeared feasible to assume that also the functional link between RboH and auxin signalling might be conserved. We therefore probed the effect of the natural auxin IAA on palmella formation (Fig. 7B) and observed that in the absence of nsPEFs, the transition into the palmella stage was strongly suppressed, consistent with the implication of our model that the ground level of superoxide (generated by RboH) was consumed for auxin signalling and therefore was not able to trigger the developmental response (transition into the palmella stage). However, the induction of palmella formation in response to nsPEFs treatment could not be quelled by the preceding application of auxin. It might be possible that the sensitivity of *C. reinhardtii* to auxin is lower than in higher plants, such that higher auxin concentrations might be required to suppress nsPEFs-dependent palmella formation. However, the observation that the concentration of auxin was sufficient to regulate proliferation and expansion, speaks against this possibility. The alternative model would be a second signal, which is deployed by nsPEFs and which is independent from oxidative burst. A possible mechanism might be other cellular targets of calcium influx through the nanopores, which in future studies could be addressed using fluorescent calcium dyes. This is feasible, since in addition to the calcium-dependent protein kinases that transduce the calcium signal into an activation of NADPH oxidase [56], there are numerous other calcium binding proteins that can read out the calcium signal into different downstream responses (for review see [61]).

5.3.1. Outlook: modulation of gene expression by nsPEFs

The still unknown signal that is released by nsPEFs unfolds its effect only several days later, and therefore must be very stable. This signal obviously persists over several rounds of cell division, which means that it has to be regenerated during each cycle to remain stable. A mere alteration of the membrane induced by nsPEFs should be diluted by a factor of 2 during each cell cycle. A candidate for such a mechanism would be stable alterations of chromatin structure leading to changes in gene expression. In this context, it would also be rewarding to analyse potential changes in the composition of membrane lipids in response to nsPEFs, but also in response to the oxidative stress imposed by salinity. Future work will therefore be directed to measure the response of gene expression to nsPEFs and to understand the epigenetic changes underlying such responses.

6. Conclusions

We have investigated the role of oxidative burst for the cellular responses induced by nsPEFs, both, short-term and long term nsPEFs. We found that nsPEFs could induce a rapid and transient increase of membrane permeability, followed by a transient volume increase, and slower lipid peroxidation. Furthermore, these responses were enhanced when the pulse duration increased from 25 ns to 50 ns. When the long-term response to nsPEFs were investigated, we observed an arrest of the cell cycle, a stimulation of cell expansion and a stimulated formation of palmella stages, correlated with a persistent long-term increasing of lipid peroxidation. While the spontaneous formation of palmella stages could be suppressed by exogenous IAA, the palmella formation in response to nsPEFs was not responsive to exogenous auxin. Our data show that nsPEFs release a long-lasting signal that persists, although the immediate cellular changes to the treatment are mostly reversed in the first two hours after pulsing. This persistent signal becomes manifest only days later and orchestrates a developmental reprogramming, which under natural conditions functions in the context of osmotic adaptation.

Transparency document

The Transparency document associated with this article can be found, in the online version.

Acknowledgments

This work was supported by a fellowship from the Chinese Scholarship Council (CSC) to Fan Bai, and funds from the Baden-Württemberg Foundation (U17) to Wolfgang Frey.

References

[1] C. Chen, S.W. Smye, M.P. Robinson, J.A. Evans, Membrane electroporation theories: a review, Med. Biol. Eng. Comput. 44 (2006) 5–14.
[2] L.M. Mir, S. Orlowski, J. Belehradek Jr., C. Paoletti, Electrochemotherapy potentiation of antitumour effect of bleomycin by local electric pulses, Eur. J. Cancer. Clin. Oncol. 27 (1991) 68–72.
[3] M. Breton, L. Delemotte, A. Silve, L.M. Mir, M. Tarek, Transport of siRNA through lipid membranes driven by nanosecond electric pulses: an experimental and computational study, J. Am. Chem. Soc. 134 (2012) 13938–13941.
[4] M. Goettel, C. Eing, C. Gusbeth, R. Straessner, W. Frey, Pulsed electric field assisted extraction of intracellular valuables from microalgae, Algal Res. 2 (2013) 401–408.
[5] P.C. Wouters, J.P.P.M. Smelt, Inactivation of microorganisms with pulsed electric fields: potential for food preservation, Food Biotechnol. 11 (1997) 193–229.
[6] K.H. Schoenbach, R.P. Joshi, J.F. Kolb, N. Chen, M. Stacey, P.F. Blackmore, E.S. Buescher, S.J. Beebe, Ultrashort electrical pulses open a new gateway into biological cells, Proc. IEEE 92 (2004) 1122–1137.
[7] N. Chen, K.H. Schoenbach, J.F. Kolb, R. James Swanson, A.L. Garner, J. Yang, R.P. Joshi, S.J. Beebe, Leukemic cell intracellular responses to nanosecond electric fields, Biochem. Biophys. Res. Commun. 317 (2004) 421–427.
[8] I. Semenov, S. Xiao, A.G. Pakhomov, Primary pathways of intracellular Ca^{2+} mobilization by nanosecond pulsed electric field, Biochim. Biophys. Acta Biomembr. 1828 (2013) 981–989.

[9] A.G. Pakhomov, S. Xiao, O.N. Pakhomova, I. Semenov, M.A. Kuipers, B.L. Ibey, Disassembly of actin structures by nanosecond pulsed electric field is a downstream effect of cell swelling, Bioelectrochemistry 100 (2014) 88–95.
[10] T. Berghöfer, C. Eing, B. Flickinger, P. Hohenberger, L.H. Wegner, W. Frey, P. Nick, Nanosecond electric pulses trigger actin responses in plant cells, Biochem. Biophys. Res. Commun. 387 (2009) 590–595.
[11] W. Ren, S.J. Beebe, An apoptosis targeted stimulus with nanosecond pulsed electric fields (nsPEFs) in E4 squamous cell carcinoma, Apoptosis 16 (2011) 382–393.
[12] G.A.D. Miller, N. Suzuki, S. Ciftci-Yilmaz, R.O.N. Mittler, Reactive oxygen species homeostasis and signalling during drought and salinity stresses, Plant Cell Environ. 33 (2010) 453–467.
[13] M.C. Mehdy, Active oxygen species in plant defense against pathogens, Plant Physiol. 105 (1994) 467–472.
[14] S. Bhattacharjee, Reactive oxygen species and oxidative burst: roles in stress, senescence and signal transduction in plants, Curr. Sci. 89 (2005) 1113–1121.
[15] P. Wojtaszek, Oxidative burst: an early plant response to pathogen infection, Biochem. J. 322 (1997) 681–692.
[16] A. Fehér, K. Ötvös, T.P. Pasternak, A.P. Szandtner, The involvement of reactive oxygen species (ROS) in the cell cycle activation (G0-to-G1 transition) of plant cells, Plant Signal. Behav. 3 (2008) 823–826.
[17] H. Sauer, M. Wartenberg, J. Hescheler, Reactive oxygen species as intracellular messengers during cell growth and differentiation, Cell. Physiol. Biochem. 11 (2001) 173–186.
[18] R. Tenhaken, A. Levine, L.F. Brisson, R.A. Dixon, C. Lamb, Function of the oxidative burst in hypersensitive disease resistance, Proc. Natl. Acad. Sci. 92 (1995) 4158–4163.
[19] G. Noctor, C.H. Foyer, Ascorbate and glutathione: keeping active oxygen under control, Annu. Rev. Plant Physiol. Plant Mol. Biol. 49 (1998) 249–279.
[20] G. Loschen, A. Azzi, L. Flohé, Mitochondrial H_2O_2 formation: relationship with energy conservation, FEBS Lett. 33 (1973) 84–88.
[21] H.J. Forman, A. Boveris, Superoxide radical and hydrogen peroxide in mitochondria, Free Radic. Biol. Med. 5 (1982) 65–90.
[22] M. Sagi, Production of reactive oxygen species by plant NADPH oxidases, Plant Physiol. 141 (2006) 336–340.
[23] X.J. Xia, Y.H. Zhou, K. Shi, J. Zhou, C.H. Foyer, J.Q. Yu, Interplay between reactive oxygen species and hormones in the control of plant development and stress tolerance, J. Exp. Bot. 66 (2015) 2839–2856.
[24] B. Varghese, S.C. Naithani, Oxidative metabolism-related changes in cryogenically stored neem (*Azadirachta indica* A. Juss) seeds, J. Plant Physiol. 165 (2008) 755–765.
[25] H.M. Wu, O. Hazak, A.Y. Cheung, S. Yalovsky, RAC/ROP GTPases and auxin signaling, Plant Cell 23 (2011) 1208–1218.
[26] X. Chang, M. Riemann, Q. Liu, P. Nick, Actin as deathly switch? How auxin can suppress cell-death related defence, PLoS One 10 (2015)http://dx.doi.org/10.1371/journal.pone.0125498.
[27] P. Hohenberger, C. Eing, R. Straessner, S. Durst, W. Frey, P. Nick, Plant actin controls membrane permeability, Biochim. Biophys. Acta Biomembr. 1808 (2011) 2304–2312.
[28] N. Sabri, B. Pelissier, J. Teissie, Electropermeabilization of intact maize cells induces an oxidative stress, Eur. J. Biochem. 238 (1996) 737–743.
[29] E. Erickson, S. Wakao, K.K. Niyogi, Light stress and photoprotection in *Chlamydomonas reinhardtii*, Plant J. 82 (2015) 449–465.
[30] J.D. Rochaix, *Chlamydomonas reinhardtii* as the photosynthetic yeast, Annu. Rev. Genet. 29 (1995) 209–230.
[31] J.D. Rochaix, Chlamydomonas, a model system for studying the assembly and dynamics of photosynthetic complexes, FEBS Lett. 529 (2002) 34–38.
[32] C.D. Silflow, P.A. Lefebvre, Assembly and motility of eukaryotic cilia and flagella. Lessons from *Chlamydomonas reinhardtii*, Plant Physiol. 127 (2001) 1500–1507.
[33] P. Spolaore, C. Joannis Cassan, E. Duran, A. Isambert, Commercial applications of microalgae, J. Biosci. Bioeng. 101 (2006) 87–96.
[34] K. Skjånes, C. Rebours, P. Lindblad, Potential for green microalgae to produce hydrogen, pharmaceuticals and other high value products in a combined process, Crit. Rev. Biotechnol. 33 (2012) 172–215.
[35] G. Gloeckner, C.F. Beck, Genes involved in light control of sexual differentiation in *Chlamydomonas reinhardtii*, Genetics 141 (1995) 937–943.
[36] A.R. Cross, O.T.G. Jones, The effect of the inhibitor diphenylene iodonium on the superoxide-generating system of neutrophils, Biochem. J. 237 (1986) 111–116.
[37] T. Proschold, Portrait of a species: *Chlamydomonas reinhardtii*, Genetics 170 (2005) 1601–1610.
[38] E.H. Harris, The Chlamydomonas Sourcebook: A Comprehensive Guide to Biology and Laboratory Use, Academic Press, San Diego California, 1989.
[39] C.J. Eing, S. Bonnet, M. Pacher, H. Puchta, W. Frey, Effects of nanosecond pulsed electric field exposure on *Arabidopsis thaliana*, IEEE Trans. Dielectr. Electr. Insul. 16 (2009) 1322–1328.
[40] S. Kühn, Q. Liu, C. Eing, W. Frey, P. Nick, Nanosecond electric pulses affect a plant-specific kinesin at the plasma membrane, J. Membr. Biol. 246 (2013) 927–938.
[41] D.F. Gaff, O. Okong'O-Ogola, The use of non-permeating pigments for testing the survival of cells, J. Exp. Bot. 22 (1971) 756–758.
[42] R.A.J. Hodgson, J.K. Raison, Lipid peroxidation and superoxide dismutase activity in relation to photoinhibition induced by chilling in moderate light, Planta 185 (1991) 215–219.
[43] J. Bereiter Hahn, Do we age because we have mitochondria? Protoplasma 251 (2013) 3–23.
[44] D. Marino, C. Dunand, A. Puppo, N. Pauly, A burst of plant NADPH oxidases, Trends Plant Sci. 17 (2012) 9–15.
[45] L.M. Henderson, J.B. Chappell, Dihydrorhodamine 123: a fluorescent probe for superoxide generation? Eur. J. Biochem. 217 (1993) 973–980.
[46] C. Triantaphylidès, M. Havaux, Singlet oxygen in plants: production, detoxification and signaling, Trends Plant Sci. 14 (2009) 219–228.
[47] D.R. Janero, Malondialdehyde and thiobarbituric acid-reactivity as diagnostic indices of lipid peroxidation and peroxidative tissue injury, Free Radic. Biol. Med. 9 (1990) 515–540.
[48] P. Campanoni, Auxin-dependent cell division and cell elongation. 1-naphthaleneacetic acid and 2,4-dichlorophenoxyacetic acid activate different pathways, Plant Physiol. 137 (2005) 939–948.
[49] O.N. Pakhomova, V.A. Khorokhorina, A.M. Bowman, R. Rodaitė-Riševičienė, G. Saulis, S. Xiao, A.G. Pakhomov, Oxidative effects of nanosecond pulsed electric field exposure in cells and cell-free media, Arch. Biochem. Biophys. 527 (2012) 55–64.
[50] K. Kinosita, T.Y. Tsong, Formation and resealing of pores of controlled sizes in human erythrocyte membrane, Nature 268 (1977) 438–441.
[51] O.M. Nesin, O.N. Pakhomova, S. Xiao, A.G. Pakhomov, Manipulation of cell volume and membrane pore comparison following single cell permeabilization with 60- and 600-ns electric pulses, Biochim. Biophys. Acta Biomembr. 1808 (2011) 792–801.
[52] K. Komsic-Buchmann, L. Wöstehoff, B. Becker, The contractile vacuole as a key regulator of cellular water flow in *Chlamydomonas reinhardtii*, Eukaryot. Cell 13 (2014) 1421–1430.
[53] J. Wolfe, M.F. Dowgert, P.L. Steponkus, Mechanical study of the deformation and rupture of the plasma membranes of protoplasts during osmotic expansions, J. Membr. Biol. 93 (1986) 63–74.
[54] B. Flickinger, T. Berghöfer, P. Hohenberger, C. Eing, W. Frey, Transmembrane potential measurements on plant cells using the voltage-sensitive dye ANNINE-6, Protoplasma 247 (2010) 3–12.
[55] L.H. Wegner, B. Flickinger, C. Eing, T. Berghöfer, P. Hohenberger, W. Frey, P. Nick, A patch clamp study on the electro-permeabilization of higher plant cells: supraphysiological voltages induce a high-conductance, K^+ selective state of the plasma membrane, Biochim. Biophys. Acta Biomembr. 1808 (2011) 1728–1736.
[56] U. Dubiella, H. Seybold, G. Durian, E. Komander, R. Lassig, C.P. Witte, W.X. Schulze, T. Romeis, Calcium-dependent protein kinase/NADPH oxidase activation circuit is required for rapid defense signal propagation, PNAS 110 (2013) 8744–8749.
[57] H.I. Anderberg, J.Å. Danielson, U. Johanson, Algal MIPs, high diversity and conserved motifs, BMC Evol. Biol. 11 (2011) 110.
[58] D. Sahoo, J. Seckbach, The Algae World, Springer, Berlin Heidelberg New York, 2015.
[59] A.J. Nappi, E. Vass, Hydroxyl radical production by ascorbate and hydrogen peroxide, Neurotox. Res. 2 (2000) 343–355.
[60] I. De Smet, U. Voß, S. Lau, M. Wilson, N. Shao, R.E. Timme, R. Swarup, I. Kerr, C. Hodgman, R. Bock, M. Bennett, G. Jürgens, T. Beeckman, Unraveling the evolution of auxin signaling, Plant Physiol. 155 (2011) 209–221.
[61] J. Kudla, O. Batistič, K. Hashimoto, Calcium signals: the lead currency of plant information processing, Plant Cell 22 (2010) 541–563.